COMPDYN 2013
4th ECCOMAS Thematic Conference on
Computational Methods in Structural Dynamics and Earthquake Engineering
M. Papadrakakis, N.D. Lagaros, V. Plevris (eds.)
Kos Island, Greece, 12–14 June 2013

STRUCTURAL MODELLING ISSUES IN SEISMIC PERFORMANCE ASSESSMENT OF INDUSTRIAL STEEL BUILDINGS

G. Della Corte[1], I. Iervolino[1], and F. Petruzzelli[1]

[1] Università degli Studi di Napoli Federico II
Via Claudio 21, 80125 Napoli
e-mail: {gaetano.dellacorte,iunio.iervolino,fabio.petruzzelli}@unina.it

Keywords: Dynamic Analysis, Risk Assessment, Seismic Response, Steel Structures.

Abstract. *The paper presents part of a study on the probabilistic seismic performance assessment of an existing industrial facility featuring a steel structure as the main building. The building is located in central Italy and is composed of structures having different construction ages. One portion was designed and built in the early 1970s and expanded in the late 1970s. In the early 1990s, a new portion was built close to the former but separated by means of gaps. All the structures are very similar in concept, though they are different in detailing and structural behavior. Six models were built up for the existing structures, four two-dimensional (2D) and two three-dimensional (3D) models. The four 2D models represent four distinct frames, one per each of the two main plan directions of the two structures (the older, i.e. the 1970s', and the newer, i.e. the 1990s'). The two 3D models are variants of a model of the newer building: the difference is the modeling options of roof truss joints. Non-linear dynamic analyses of the six structural models were carried out. Ground acceleration records were specifically selected consistent with disaggregation of seismic hazard at the site. The probability distribution of demands was then investigated, considering both global and local failure modes. This paper, in particular, presents and discusses results for only the global response assessment, in terms of peak transient and residual roof drifts. The structural modeling issues are discussed with a focus on the effects that different modeling options may have on assessment of seismic fragility and risk. The main conclusions drawn are: (i) roof truss failure might occur in the form of instability of a group of members, a failure mode – triggered by local out-of-plane truss vibrations and P-Delta effects – that can be only captured by a 3D model; (ii) including residual drifts, along with peak transient values, in the evaluation of the probability of failure can be of utmost importance if the structure is relatively stiff (thus experiencing small peak drift) but weak (thus easily experiencing inelasticity). The first conclusion above is specific for industrial steel buildings but applicable to all those characterized by a roof truss with the possibility of out-of-plane joint displacements, while the second conclusion appears to have general validity for the seismic risk assessment of structures.*

1 INTRODUCTION

The industrial building stock of many countries is significantly contributed by steel structures. Although the latter are generally relatively lightweight structures and, in most of cases, designed for wind actions, the assessment of their seismic performance is important for the estimation of the possible consequences of earthquakes, in terms of direct damage and/or business interruption. On the other hand, it is known that assessing the performance of existing structures is a task quite different with respect to the design of a new one. An especially relevant issue is the need for models to be able to capture all the potential failure modes, especially those reflecting brittle behavior. Old steel structures are frequently characterized by partial-strength connections, whose contribution to the system's inelastic response cannot be neglected. In the special case of industrial steel buildings, the undesired failure modes may involve also the roof structure, whose design is generally dominated by gravity and wind loading. Besides, the roof structure is frequently a complex three-dimensional system, whose dynamics may involve modes of failure different from the case of horizontal rigid floor diaphragms.

The analysis of the above issues was tackled in the study presented in the following, within the context of probabilistic risk assessment and performance-based earthquake engineering. The study was carried out with reference to a case study industrial steel building, which is characterized by constructional details (columns, connections, roof members, roof bracing) that are common for this structural type. Therefore, investigations may allow tracing comments and drawing conclusions applicable to similar structures.

The following Sections give first a short description of the building structures and of the models set-up. Subsequently, seismic hazard at the building site is described by means of results from a site-specific probabilistic seismic hazard analysis (PSHA); ground motion records were consequently selected from available databases. The selected ground motions were then used to analyze seismic demands to the investigated building structures. Results from nonlinear dynamic analyses of multiple two-dimensional (2D) and three-dimensional (3D) structural models are presented and commented in this paper with reference to structural fragility and seismic risk represented by means of annual failure probability.

2 THE BUILDING STRUCTURES

Figure 1a shows an aerial view of the whole building, while Figure 1b illustrates schematically the structural plan layout. There are four building structures, separated by gaps. The white area in Figure 1b refers to the oldest structure, built in 1971 and separated into two portions by a longitudinal joint parallel to the direction X. In 1979 these two portions were enlarged with no separation between the new and old constructions (light grey shaded area in Figure 1b). Considering that additions were built using the same materials and structural dimensions as those of the previous 1971 structures, these will be referred to as 1971/79 structures. Finally, the most recent parts were built in 1991, as indicated by the dark grey shadow in Figure 1b. Both the 1971/79 and the 1991 structures were designed according to old seismic codes [1], with significant underestimation of design seismic intensities with respect to current design seismic actions based on probabilistic hazard at the site. Codes and Standards used for the design of the existing structures were based on the *Allowable Stress* method without any account of *Capacity Design* principles. The latter were in fact enforced only very recently [2] for the Italian design professionals. The expected consequence is that no control was taken of the location of plastic zones, which may therefore involve also relatively brittle failure modes.

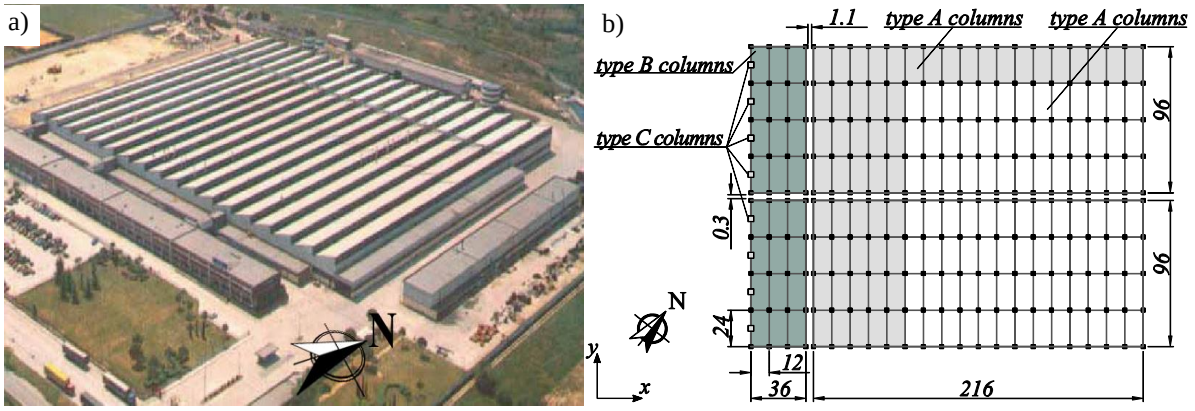

Figure 1: Aerial view of the whole facility (a) and schematic drawing illustrating the plan layout (units: m) (b).

Parts made in different years have similar columns and roof structures. The latter are made of shed-type trusses in direction X and Pratt trusses in direction Y. Sample structural cross sections of trusses in directions X and Y, as recorded in the original design drawings, are reproduced in Figures 2a, 2b and 2c. Figures 2a and 2b show typical cross sections of roof trusses for internal frames. Figure 2c shows a cross section of the truss located onto the south-west side perimeter frame. Such a perimeter frame is characterized by additional columns with respect to other frames (Fig. 1b), and a smaller free length of columns because the corresponding roof truss is at a smaller height (Fig. 2c). A sample of some details of roof joints is illustrated in Figure 2d. As mentioned, detailing (bolts pitch, hole-to-bolt diameter tolerance, etc.) follows outdated Italian regulations about the design of steel structures [1]. The roof structure is completed by in-plane sub-horizontal X-bracing and minor elements supporting the roof panels.

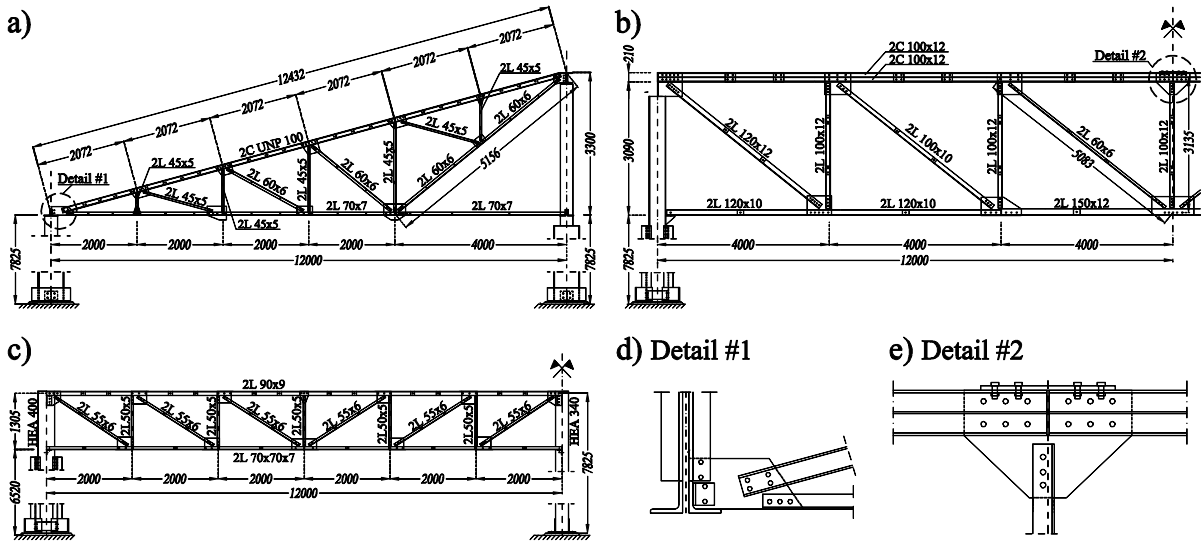

Figure 2: Sample structural cross-sections of trusses in direction X (a) and Y (b, c); sample (qualitative) details of roof member joints (d).

Vertical resisting members, which are both sustaining the roof structure and resisting horizontal forces, are composite battened columns. In the portions of the structure built in 1971/79, composite columns are made of two IPE 360 shapes, reinforced on the flanges with 15 mm thick plates and coupled together by battens consisting of plates welded to the flanges of the two profiles (Fig. 3a). A HE A 240 shape is welded at the top-end of the battened column in

order to connect the roof trusses. These composite columns will be hereafter referred to as columns of type A, whose plan location is shown in Figure 1b. In the 1991 building, the main columns, referred to as type B (Fig. 1b), are also composite members, obtained by battening IPE 600 shapes. Battens of type-B columns were obtained by cutting pieces from hot-rolled profiles with HE A 500 cross-section and bolting their flanges to the web of the main column members, as shown in Figure 3b. A hot-rolled HE A 400 shape is placed at the top-end of the column, connecting the latter to the roof trusses. Flanges of the HE A 400 shape are connected to the web of the composite column members by means of bolts, as made for battens (Fig. 3c). In addition to the above, there are also columns consisting of a single hot-rolled HE A 340 shape (type C, Fig. 3d), located at the left-hand side perimeter frame shown in Figures 1b and 2c. These type-C columns are located in the middle of each main span, whose length is therefore reduced to one-half (12 m) of the value in other frames parallel to the direction Y.

Figure 3 also shows details of the connections to the foundation for different types of columns. For type A columns (Fig. 3a), the connection is provided by a single 20 mm thick steel plate with four anchor bolts (diameter = 30 mm). For type B columns (Fig. 3b), the connection is constituted of two distinct 30 mm thick base plates, each one with three anchor bolts (diameter = 30 mm). The connection of type C columns to the foundation (Fig. 3d) is comprised of a steel plate (thickness = 30 mm) and four anchor bolts (diameter = 30 mm). In each of the cases described above, base plate stiffeners with thickness varying between 15 and 20 mm were used.

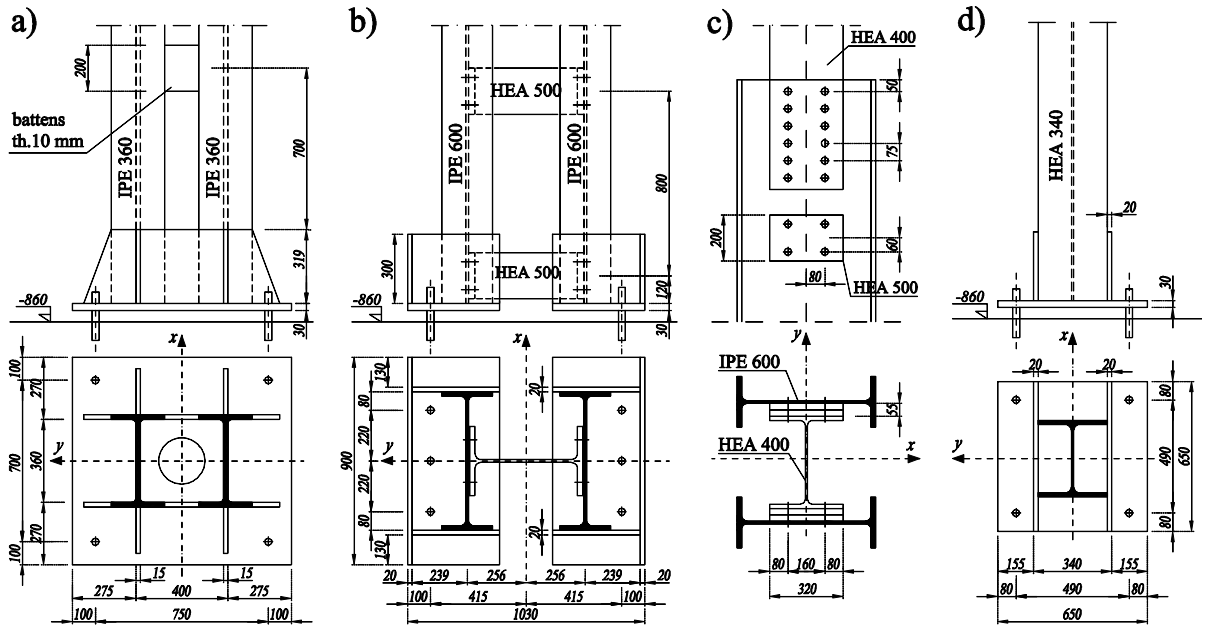

Figure 3: Columns and base connections: a) type A, b) type B, c) details at the top of type B columns, d) type C.

Based on the available information, it is inferred that building foundations are made of isolated reinforced concrete blocks. Original design documents indicate that the soil can be assumed as class B according to the Italian Seismic Code [2]. Soil type B is a quite stiff soil, which is characterized by average shear wave velocity in the first 30 m of depth from ground surface ($V_{S,30}$) in the range 360 m/s to 800 m/s. Soil-structure interaction is expected to be not significant for such soil conditions and it was neglected in the analysis.

As-built data collection is always important for a reliable assessment of the performance of existing constructions. Generally, expected average material properties are used to evaluate the seismic strength and to estimate the seismic deformation demand. According to the cur-

rent Italian seismic code [2], the expected average values of steel yield strength are about 1.10-1.20 times the characteristic values, depending on the grade. No information is provided by the code about average-to-characteristic strength ratio of bolts, which are considered non-dissipative elements for the design of new structures. However, as shown in the next Sections, in the case study structures as-built column base connections are partial-strength. Column base connection failure occurs with a mixed failure mode involving failure of bolts in tension. Therefore, a necessary (but cautious) modeling choice was to use the characteristic strength of bolts in the calculation of column base connection strength. In order to be consistent with the use of characteristic values of bolt strength, it was decided to use always the characteristic value of material strengths. The latter, due to the relatively small variability of yield strength, is close to the mean value and therefore it is expected to have a minor effect on the bias in the failure probability as computed in Section 6. However, to check the eventual occurrence of some failure modes (e.g., failure of base plate welds or failure of column battens), peak values of column base strength were estimated using commonly adopted material and strain-hardening factors, with a total overstrength factor assumed equal to about 1.3. The original design documents report the following characteristic values of the material strengths: yield strength of members f_{ym} = 235 MPa; yield strength of column base plates f_{yp} = 275 MPa; yield strength of roof gusset plates f_y = 355 MPa; grade 8.8 for bolts; grade C20/25 for concrete [3].

3 STRUCTURAL MODELS

This Section highlights a few aspects relevant to the modeling for seismic performance assessment of the case study structures. Figure 4 illustrates schematically the numerical models: four two-dimensional (2D) frame models, one per direction (X and Y) for each of the structures built in 1971/79 and 1991; two three-dimensional (3D) models for the 1991 building, here analyzed for earthquakes acting along direction Y. The two 3D models built up for the 1991 building structure are differing for the modeling hypotheses of roof truss joints, as further discussed in the following.

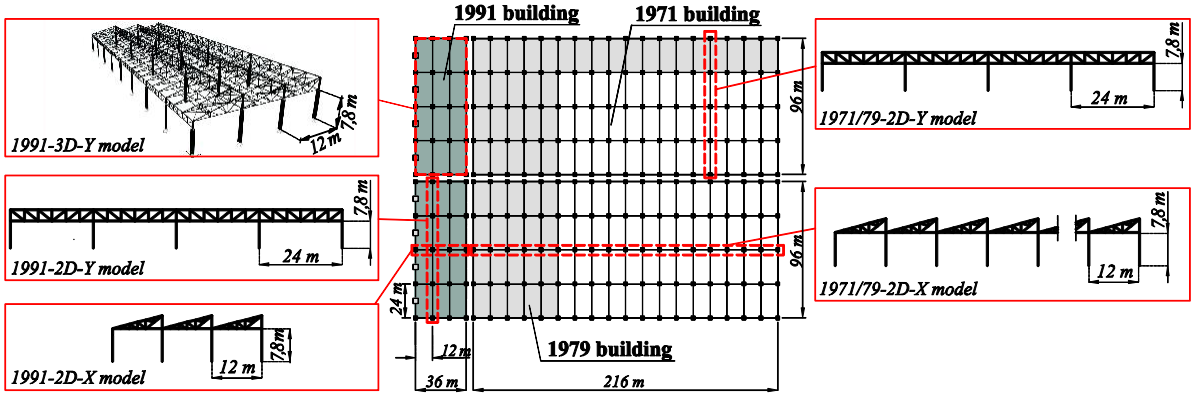

Figure 4: Structural models for 1991 and 1971/79 portions of the case study buildings.

The 1991 structures are characterized by the type B column base connections (Fig. 3b), which are appreciably different from the standard types covered by Eurocode 3 (EC3) [3]. However, using the same principles at the basis of the EC3 *component method*, but slightly adapting/interpreting the rules given in the code, component contributions to the total rotational stiffness and strength were derived [4].

An issue common to all the investigated numerical models is the representation of the hysteresis response of plastic zones, especially with reference to cyclic degradation phenomena. Previous studies [5, 6, 7] have shown that in-cycle strength degradation, such as the one due

to P-Delta effects, has a much more pronounced effect on the evaluation of seismic response than cyclic strength degradation, especially for flexible structures. Generally, the development of accurate models representing the hysteretic response of plastic zones involves significant efforts, even in case of standard geometries for which several experimental results are available. In the specific case studies, column base connections of type B are characterized by geometry for which there are no experimental test results available. Based on the above arguments, the cyclic moment-rotation response of column base connections was approximated by the *Pivot* hysteresis model [8] including pinching of hysteresis loops but no cyclic degradation. The moment-rotation response of flexural plastic hinges in hot rolled members was approximated by an elastic-perfectly-plastic model.

Failure of battens in composite columns was checked to be not a concern by verifying that they were able to sustain the maximum internal actions corresponding to the peak column shear force associated with the flexural strengths at the top and bottom ends. Consequently, composite columns were treated as linear elastic elements, taking into account the increase of shear elastic deformability due to the discontinuous and flexible web connections [3].

It is finally to remark that pounding of adjacent frames was not explicitly modeled, because displacement demand from the analysis of individual frame models (Section 5) showed that relative joint displacements would never be large enough to close the existing gap prior to the occurrence of global frame collapse.

3.1 3D vs. 2D models

The behavior of single-storey industrial steel buildings is generally affected by the roof deck diaphragm, which is almost always comprised of a thin-walled cold-formed trapezoidal sheet. The shear flexibility of such deck diaphragm is not negligible, generally leading to an increase of the building period of vibration with respect to a model based on rigid diaphragm assumption [9]. However, it has also been proved that nonstructural components may reduce appreciably the period of vibration with respect to predictions based on a model including the steel deck only [10]. It is noted that the contribution of nonstructural components may be difficult to be quantified in practice. On the other hand, a typical practice in the design consists of neglecting the stiffening contribution of the roof deck diaphragm while using roof braces, an option also selected for the case study building. However, such roof braces are characterized by high slenderness leading to buckling for relatively low levels of seismic intensity. Whether roof braces buckle, the coupling of response of parallel 2D frames obviously reduces and the system response approaches the one of isolated 2D frames. In addition, consideration has to be given to the feature of a 3D model to explicitly and automatically capture buckling of the roof structure. 2D models are unable to represent out-of-plane buckling of the roof trusses and they therefore may be missing important information about the possible failure modes of the structure. Out-of-plane buckling modes are sensitive to end-restraint conditions. Members of roof trusses are commonly modeled as perfectly pinned at their ends when in-plane structural analysis is to be carried out. This is generally motivated because the truss response is dominated by axial forces: neglecting bending moments removes one source of stiffness and strength thus resulting into conservative global response assessment. However, out-of-plane end-restraints may be essential in case of transverse vibrations of plane trusses: releasing transverse end moments may result in such a case into an unstable structure.

Therefore, the issue of 3D versus 2D model predictions has been investigated. In particular, the importance of modeling of roof joints was investigated by analyzing two alternative 3D models: (i) a model where all roof joints were assumed to be fully continuous (labeled as *fully continuous*) and (ii) a model where all moments were released for those members interrupting at a joint (labeled as *partially continuous*). Results from analyses of 3D models are subse-

quently also compared with those from 2D models, which have the advantage of being much less cumbersome from the points of view of the computational time and effort. In the 3D model the roof bracing elements were assumed to be linear elastic but with P-Delta effects activated. Therefore, the 3D model is able to capture elastic buckling but it is not able to capture inelastic buckling or failure of connections, which must be checked separately based on peak force demand.

4 SEISMIC HAZARD AND GROUND MOTIONS

The site of interest (that cannot be disclosed for confidentiality) is located in central Italy, in the middle of Appennines and its seismic hazard was computed ad-hoc. In fact, although hazard is made available by the *Istituto Nazionale di Geofisica e Vulcanologia* (INGV) [11] for a dense grid covering the country, such an information is only for site class A (rock), which does not correspond to the local geological conditions of the facility. Therefore, hazard curves were computed via the software described by Convertito *et al.* [12], employing the seismic source zone model for Italy of Meletti *et al.* [13]; the latter is also adopted for the official nationwide hazard assessment by INGV. The parameters associated to each of the zones in terms of minimum and maximum magnitude, rate of occurrence, and b-value of the Gutenberg-Richter relationships, were given by Barani *et al.* [14].

For the purposes of dynamic structural analysis, the spectral accelerations at the fundamental period of the structures and 5% damping ratio, $S_a(T_1)$, have been adopted as the ground motion intensity measures (IMs). Therefore, specific hazard curves for 1 s and 1.6 s (the fundamental periods of the 1991 and 1971/79 structures, respectively) were developed for *stiff soil* considered as a proxy for B-type site class. The resulting hazard curves are given in Figure 5 and served as a basis for the risk assessment discussed in Section 6.

In fact, hazard was also used, via disaggregation, for ground motion (GM) record selection. Disaggregation was carried out in terms of magnitude, M, and source-to-site distance, R. Disaggregation changes with the IM-value considered and therefore with the return period T_R. To cover a wide range of IM-values, the hazard for four levels of $S_a(1s)$, corresponding to 50, 475, 975 and 2475 yrs. return periods, was disaggregated. This allowed to determine the *design earthquakes* for each T_R and both IMs, using the same procedure as in Iervolino *et al.* [15]. Table 1 reports the M and R bins and strong motion databases in which records were selected via the REXEL software [16]. Sets of 30 one-component records were selected for each bin [4]. These sets were employed as an input for incremental dynamic analysis (IDA) [17] at intensity levels around that of the return period they correspond to [4]. The records of the selected sets were scaled in a way the elastic spectral acceleration at the fundamental period of vibration of each structure is equal to the target intensity level in all the IDA steps.

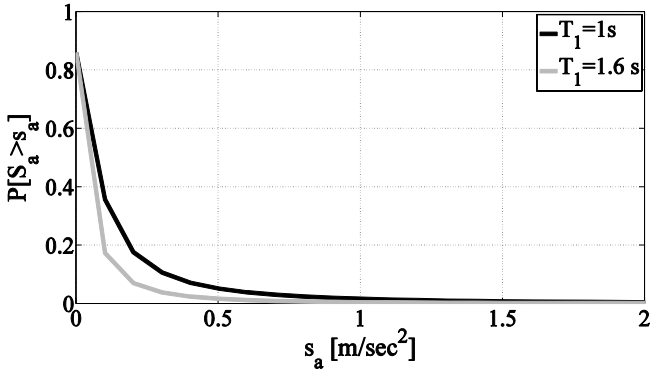

Figure 5: Seismic hazard for the site in terms of annual exceedance probability for the IMs of interest.

T_R [yr]	S_a(1s) [g]	R [km]	M	Database
50	0.10	0-20	5-6	ITACA
475	0.30	0-30	5.3-6.5	ITACA
975	0.37	5-25	6-7	ESD
2475	0.50	0-40	6-7.5	ESD

Table 1: Record selection bins consistent with disaggregation of seismic hazard at the facility site. ITACA is the Italian ACcelerometric Archive, and ESD is the European Strong-motion Database [16].

5 NON LINEAR DYNAMIC ANALYSES

Results of IDAs are summarized hereafter by showing the relationships between the assumed IM and the selected engineering demand parameters (EDPs). The latter were peak transient and residual roof drift ratios (ratios of displacement and corresponding height on the ground) for the global response assessment. Results were obtained using lumped plasticity finite element models analysed by means of SAP 2000 v.14 [18].

Figure 6 shows results in terms of drift ratio demand to the four 2D structures for all the selected earthquake intensities and GMs. Both peak transient (full dot) and residual (empty dot) drift demands are shown. Median drift demands are also illustrated with solid line (transient) and dashed line (residual). Figures 6a and 6b allow comparing the response of the 1971/79 frames, in the X and Y directions respectively. It is noted that the X-direction frame is characterized by an appreciable (non-zero) value of the drift under gravity loads (i.e. for $S_a = 0$). This is due to the asymmetry of the 2D frame, which is swaying laterally under gravity loading. It is also noted that at relatively small values of seismic intensity, the ratio of median residual to peak transient demand to the X-direction frame (Fig. 6a) is larger than it is for the Y-direction frame (Fig. 6b). This is an aspect having an influence on the probability to exceed a given limit state expressed either in terms of residual drift or transient drift or in terms of both quantities (see next Section). Figures 6c and 6d allow comparing the X and Y direction response of the 1991 building. Similarly to the 1971/79 frames, the ratio of residual to peak transient drift is larger for the X-direction than it is for the Y-direction frame. Differently from the 1971/79 frame, the X-direction frame is characterized by a small initial (gravity-induced) drift. This will have consequences on fragilities and probabilities of failure calculated considering both residual and transient drifts as discussed in the next Section.

Figure 7 illustrates the median drift demands to the 1991-3D-Y models. The median drift demand to the 1991-2D-Y frame is also reported in Figure 7 in order to compare the global performance predicted from 3D and 2D models. For spectral accelerations up to about 0.5g, all models show a similar median drift demand. At larger spectral accelerations the behavior changes radically. In case of a 3D model, the number of GMs inducing global collapse increases much more rapidly than it does for a 2D model. Such a large difference in response is due to the activation of a different collapse mechanism. Collapse of the 1991-2D-Y frame occurs with a column-sway mode (Fig. 8a). The same type of collapse mechanism is also exhibited by the X-direction 2D frames (Fig. 8b). The collapse mechanism of the 1991-3D-Y model is instead characterized by relatively complex three-dimensional instability of roof trusses (Fig. 8c), a mode of response which cannot be captured by 2D models. The details of the collapse mode depend on the GM, because high-frequency modes of transverse vibration of planar trusses are activated depending on the GM frequency content. Clearly, the *fully continuous* 3D model leads to a better structural response than the *partially continuous* 3D model, because roof instability is delayed at larger levels of spectral acceleration by introducing continuity of the joint bending moments. Thus, the *fully continuous* 3D model approaches the response of the 2D model for which such roof instability is *a priori* excluded.

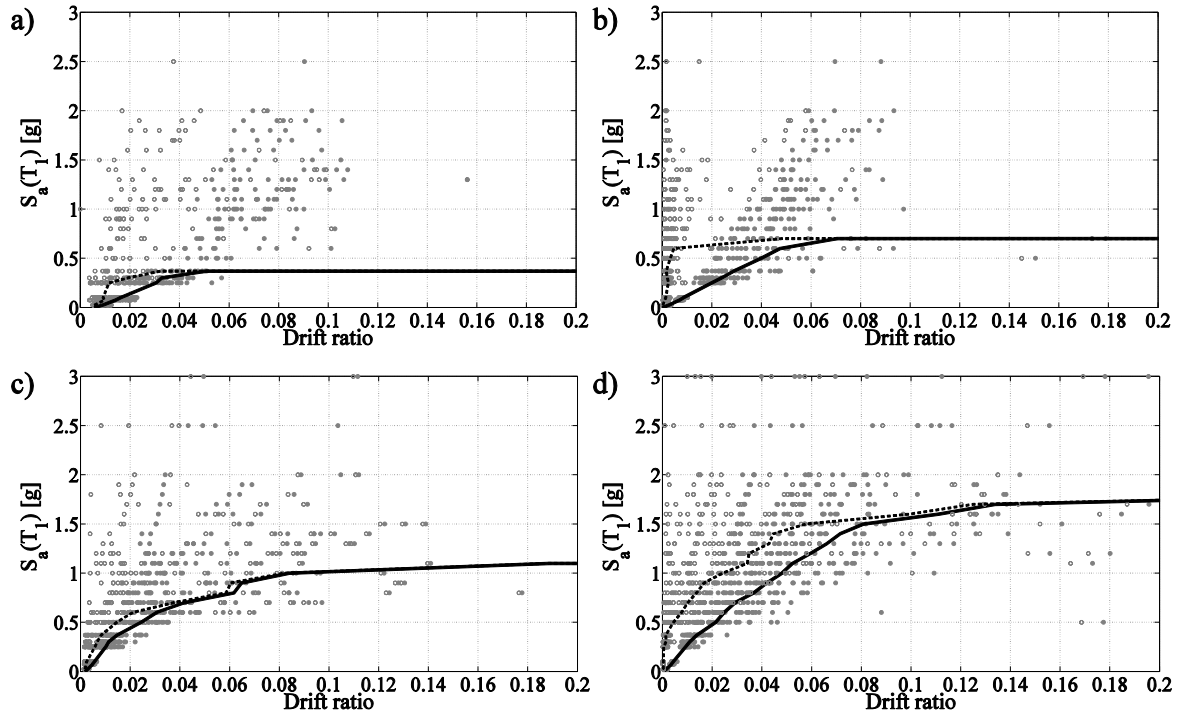

Figure 6: Peak transient and residual drift ratio for 2D frames: (a) 1971/79-2D-X; (b) 1971/79-2D-Y; (c) 1991-2D-X; (d) 1991-2D-Y.

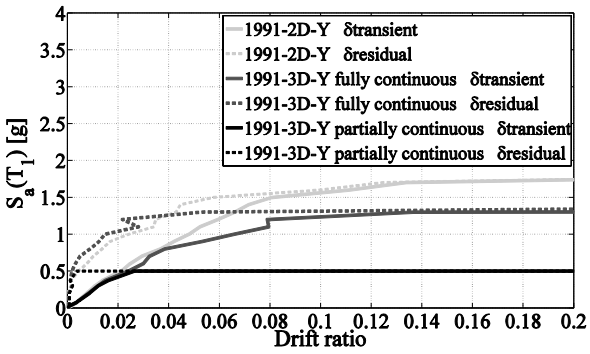

Figure 7: Peak transient drift ratio for the 1991-3D-Y models and the corresponding 1991-2D-Y frame.

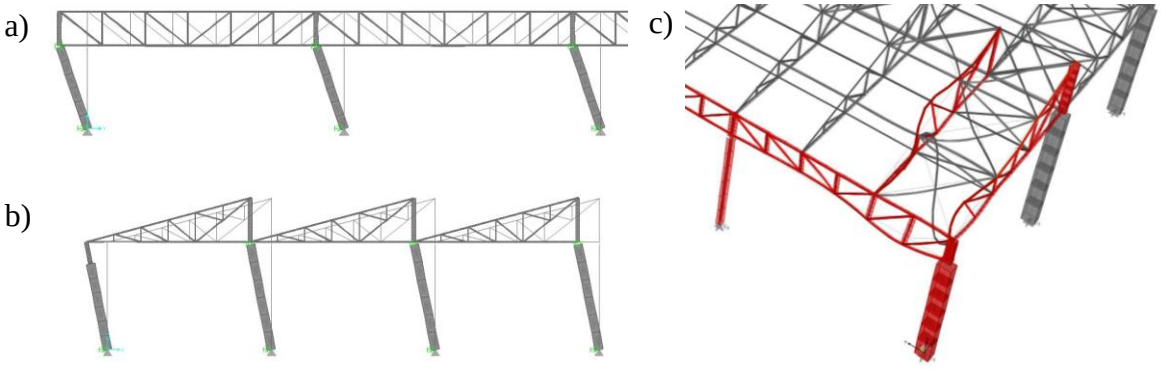

Figure 8: Collapse mechanisms: (a) 1991-2D-Y frame; (b) 1991-2D-X frame; (c) 1991-3D-Y model.

6 FRAGILITIES AND FAILURE PROBABILITIES

Three limit states were considered: Immediate Occupancy (IO), Life Safety (LS) and Collapse Prevention (CP) [19]. For global performance assessment, such limit states are defined in terms of limit values of residual drifts and/or peak transient drifts. Transient drift ratio capacities corresponding to the IO, LS and CP performance levels were assumed equal to 0.0075, 0.025 and 0.05. The residual drift ratio capacity at the CP limit state coincides with the peak transient capacity, while it was assumed equal to 0.01 at the LS limit state. According to ASCE [19], the residual drift must be *negligible* at the IO limit state. It was assumed that this means that the residual drift must be smaller than or equal to the initial drift due to gravity loading (i.e., the pre-earthquake drift). A composite rule was used to define global *collapse*, considering either numerical instability or the transient drift being larger than 0.1, a limit introduced to exclude entering a region where the model is not trustworthy [17].

Figure 9 shows example comparisons of fragility curves obtained on the basis of only the peak transient drift ratio (*univariate* distribution of demands) and those calculated considering limits on the residual drifts also (*bivariate* distribution of demands). Figure 9a shows fragilities computed for the 1971/79-2D-X frame (based on IDA results illustrated in Figure 6a), while Figure 9b is relevant to the 1991-2D-X frame (IDA results in Figure 6c). For both structures, at the CP limit state, the two types of fragility curves (for *univariate* and *bivariate* distributions) are practically coincident, because the residual drift demand is always smaller than the transient drift demand, while capacity limits [19] are coincident. The largest effect of including limitations on the residual drifts is expected to appear in the calculation of fragilities for the LS and, especially, the IO limit states. However, the changes in the calculated fragilities can be either large or small, because of the structure peculiar response. For example, Figure 9a shows no significant effect at the IO limit state, while Figure 9b shows large difference. Indeed, the 1971/79-2D-X frame is subject to a relatively large initial (gravity induced) drift (Fig. 6a). As mentioned above, such an initial drift is the assumed residual drift capacity at the IO limit state; it is relatively large and close to the peak drift capacity for the 1971/79-2D-X frame. On the other hand, median residual drift demands resulted to be relatively small with respect to median transient demands (Fig. 6a), because of the flexibility of the structure associated with large peak drifts and small inelasticity. Thus, introducing a limit to the residual drift did not change significantly the total seismic fragility of the 1971/79-2D-X frame. An opposite trend is revealed by the 1991-2D-X frame: the ratio of residual and transient drift capacity is small while the ratio of the median residual and transient drift demand is large (Fig. 6c). Consequently, the frequency of exceeding the IO limit state because of an excessive residual drift had a strong effect on the total computed fragility (Fig. 9b).

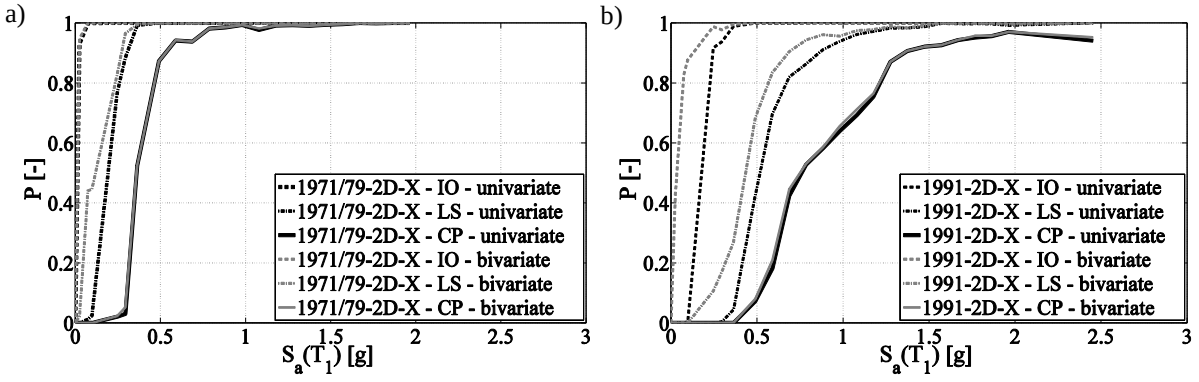

Figure 9: Fragility curves: a) 1971/79-2D-X frame; b) 1991-2D-X frame.

Given the hazard (Section 4) and the fragilities discussed above, the annual probability of failure (P_f) was computed [4]. The P_f calculated on the basis of the peak transient drifts are reported in Table 2, while Table 3 gives percentage variations obtained when also residual drifts were included in the analysis. Tables 2 and 3 permit appreciating the seismic reliability of the analyzed structures, the influence of the model adopted, as well as the importance of including residual drifts in the assessment.

Table 2 shows that that Y-direction frames are generally more reliable than X-direction frames: this is because of the larger stiffness and strength observed for Y-direction frames. It is worth remembering that this paper discusses only the global response in terms of roof drift ratios and the above conclusion is based on only such response parameters. A more comprehensive assessment must necessarily include local failure modes; e.g., failure of roof members and connections [4, 20, 21]. (It has to be noted that differences between results reported in Table 2 and those presented in [21] are generally due to refinements made to the numerical fragility curves at low levels of spectral accelerations. In addition, the 3D model previously analyzed [20] was characterized by different joint restraint modeling assumptions.)

Table 3 confirms the results of Figure 9. If transient and residual drift capacities are close each other, the inclusion of residual drifts in the calculation of P_f must obviously have a minor effect, because the residual drift demand is always smaller than the transient value. If the residual drift capacity is significantly smaller than the transient value, the influence of including residual drifts in the calculations will still depend on the distribution of demands. At a given level of spectral acceleration, if the median residual and transient drift demands are relatively similar, which is the case for stiff but weak structures, then the limit imposed to the residual drift is expected to have a remarkable influence on the calculated P_f. On the contrary, if the median transient drift demand is larger than the median residual drift demand, as in case of flexible and strong structures, the influence will be smaller though it may still be significant.

Frame	IO	LS	CP
1971/79-2D-X	3.7E-02	1.2E-03	2.0E-04
1971/79-2D-Y	5.7E-03	3.3E-04	7.0E-05
1991-2D-X	5.1E-03	4.7E-04	1.9E-04
1991-2D-Y	5.0E-03	3.9E-04	1.1E-04
1991-3D-Y “fully continuous”	5.9E-03	4.2E-04	1.7E-04
1991-3D-Y “partially continuous”	6.0E-03	4.3E-04	3.4E-04

Table 2: Probabilities of failure based on only the peak transient drift.

Frame	IO	LS	CP
1971/79-2D-X	1.26	454.30	2.74
1971/79-2D-Y	113.40	3.62	0.13
1991-2D-X	1182.59	152.06	4.97
1991-2D-Y	1.81	6.92	8.33
1991-3D-Y “fully continuous”	6.48	0.55	0.35
1991-3D-Y “partially continuous”	4.14	0.79	0.38

Table 3: Variations of probabilities of failure due to inclusion of residual drifts; the table gives the percentage differences with respect to values shown in Table 2.

7 CONCLUSIONS

This paper has presented failure mode considerations versus modeling assumptions in the probabilistic seismic global performance assessment of a case study industrial steel building.

Results of dynamic nonlinear analyses of different frame models extracted from the case study buildings have been discussed. The analyses were based on sets of ground motion records consistent with site-specific probabilistic seismic hazard analysis. Integrating the hazard and the fragility curves for different limit states, annual probabilities of failure were obtained. The following are the main conclusions drawn from the study.

- Using a 3D model highlighted the possibility of roof truss failure in the form of complex three dimensional instability modes, involving groups of roof truss members. Such failure modes cannot be predicted using 2D models, because of the intrinsic 3D features of transverse vibrations of planar trusses. The latter vibrations are triggering local P-Delta effects, which are responsible of the instability modes. This conclusion is valid for all industrial steel buildings featuring a roof truss structure with out-of-plane joint displacements.
- Including both residual and peak transient drifts in the seismic risk assessment could be either very important or rather unessential depending on the structural characteristics and the relative magnitude of limits on residual and transient drifts. Results obtained within this study suggests that, generally, residual drifts should be included in the analysis, unless it can be anticipated by clear reasoning that they would have a minor effect on the probability of failure. The results presented in this paper might be helpful in identifying the latter cases. Such comments on the influence of residual drift limitations are clearly valid beyond the specific case study of industrial buildings.

ACKNOWLEDGEMENTS

This work was partially supported by AXA-MATRIX, within the AXA-DIST 2010-2013 research program, and partially by ReLUIS, within the ReLUIS-DPC 2010-2013 research program.

REFERENCES

[1] CS.LL.PP. (1996). D.M. 16.01.1996: Norme Tecniche per le Costruzioni in Zona sismica, 29, 5 febbraio 1996 (in Italian).

[2] CS.LL.PP. (2008). D.M. 14.01.2008: Norme Tecniche per le Costruzioni. *GU della Repubblica Italiana*, 29, 4 febbraio 2008 (in Italian).

[3] CEN (2005). *EN 1993-1-1, Eurocode 3: Design of steel structures – Part 1-1: General rules and rules for buildings*. European Committee for Standardization, Brussels.

[4] F. Petruzzelli, *Scale dependent procedures for seismic risk assessment and management of industrial building portfolios*. PhD Thesis in Seismic Risk, University of Naples Federico II, Advisor: I. Iervolino, 2013.

[5] G. Della Corte, G. De Matteis, R. Landolfo, F.M. Mazzolani, Seismic analysis of MR steel frames based on refined hysteretic models of connections. *Journal of Constructional Steel Research*, **58**, 1331-1345, 2002.

[6] L.F. Ibarra, H. Krawinkler, *Global collapse of frame structures under seismic excitations.* Report No. 152, The John A. Blume Earthquake Engineering Center, Department of Civil and Environmental Engineering, Stanford University, 2005.

[7] ATC, *Improvement of nonlinear static seismic analysis procedures (FEMA 440)*. Prepared by Applied Technology Council, Redwood City, California, for Federal Emergency Management Agency, Washington, D.C., 2005.

[8] R.K. Dowell, F.S. Seible, E.L. Wilson, Pivot hysteretic model for reinforced concrete members. *ACI Structural Journal,* **95**, 607–617, 1998.

[9] R. Tremblay, C. Rogers, E. Martin, W. Yang, Analysis, testing and design of steel roof deck diaphragms for ductile earthquake resistance. *Journal of Earthquake Engineering*, **8(5)**, 775–816, 2004.

[10] S. Mastrogiuseppe, C.A. Rogers, R. Tremblay, C.D. Nedisan, Influence of nonstructural components on roof diaphragm stiffness and fundamental periods of single storey steel buildings. *Journal of Constructional Steel Research,* **64**, 214227, 2008.

[11] M. Stucchi, C. Meletti, V. Montaldo, H. Crowley, G.M. Calvi, E. Boschi, Seismic hazard assessment (2003-2009) for the Italian building code. *B. Seismol. Soc. Am.*, **101**, 1885–1911, 2011.

[12] V. Convertito, I. Iervolino, A. Herrero, The importance of mapping the design earthquake: insights for southern Italy. *Bulletin of the Seismological Society of America*, **99(5)**, 2979–2991, 2009.

[13] C. Meletti, F. Galadini, G. Valensise, M. Stucchi, R. Basili, S. Barba, G. Vannucci, E. Boschi, A seismic source zone model for the seismic hazard assessment of the Italian territory. *Tectonophysics*, **450**, 85–108, 2008.

[14] S. Barani, D. Spallarossa, P. Bazzurro, Disaggregation of probabilistic ground motion hazard in Italy. *Bulletin of the Seismological Society of America*, **99**, 2638–61, 2009.

[15] I. Iervolino, E. Chioccarelli, V. Convertito, Engineering design earthquakes from multimodal hazard disaggregation, *Soil Dynamics and Earthquake Engineering*, **31(9)**, 1212–1231, 2011.

[16] I. Iervolino, C. Galasso, E. Cosenza, REXEL: computer aided record selection for code-based seismic structural analysis. *Bulletin of Earthquake Engineering*, **8**, 339–362, 2010.

[17] D. Vamvatsikos, C.A. Cornell, Incremental dynamic analysis. *Earthquake Engineering and Structural Dynamics*, **31**, 491–514, 2002.

[18] E.L. Wilson, *Three-dimensional static and dynamic analysis of structures.* Berkeley (CA, USA). Computers & Structures, Inc., 2002.

[19] ASCE, Pre-standard and Commentary for the Seismic Rehabilitation of Buildings. *Report No. FEMA 356*. Reston, VA: American Society of Civil Engineers prepared for the Federal Emergency Management Agency, 2000.

[20] F. Petruzzelli, G. Della Corte, I. Iervolino, Seismic risk assessment of an industrial steel building. Part I: Modelling and analysis. *Proceedings of the 15th World Conference on Earthquake Engineering*, Paper No. 3088, Lisbon, Portugal, 2012.

[21] F. Petruzzelli, I. Iervolino, G. Della Corte, Seismic risk assessment of an industrial steel building. Part II: Fragility and failure probabilities. *Proceedings of the 15th World Conference on Earthquake Engineering*, Paper No. 3086, Lisbon, Portugal, 2012.